

Supplementary Material

Climate impact and energy use of structural battery composites in electrical vehicles – Comparative prospective life cycle assessment

Frida Hermansson^{1*}, Fredrik Edgren², Johanna Xu³, Leif E. Asp³, Matty Janssen¹, Magdalena Svanström¹

¹Environmental Systems Analysis, Chalmers University of Technology, 412 96 Gothenburg, Sweden

²Body Technology, Volvo Cars, 405 31 Gothenburg, Sweden

³Material and Computational Mechanics, Chalmers University of Technology, 412 96 Gothenburg, Sweden

*Corresponding author. Email: frida.hermansson@chalmers.se

STRUCTURAL BATTERY PRODUCTION	1
Negative electrode	1
Positive electrode	2
LiFePO ₄ production	3
Cellulose separator	3
Current collector	4
Casing	5
Assembly of the battery	5
LIFE CYCLE INVENTORY	6
Carbon fibre production	6
Lignin based carbon fibre production	6
LiFePO₄ production	9
Production of Structural battery electrolyte	10
Structural battery composite manufacturing	11
Conventional vehicle manufacturing	12
Mass of car parts	13
Lightweighting and avoided Li-ion battery production	14
End of life treatment	15
CRADLE-TO-GATE RESULTS	16
SENSITIVITY ANALYSIS	17
DECREASING THE USE OF CABLES	20
CHANGING ENERGY MIX	20
Traditional BEV	20
Steel	20
Nitrogen	21
Aluminium	21
Structural battery composites vehicles	21
Lignin production	22
LiFePO ₄	22
Li-ion battery	22

Use phase	23
Incineration	23
Pyrolysis	23
NET CRADLE-TO-GRAVE RESULTS	24
REFERENCES	26

Structural battery production

This inventory is for the production of a carbon fibre (CF),CF/LiFePO₄ structural battery with a cellulose separator. It is assumed that the energy density of the material is 70 Wh/kg and that the effective modulus is 70 GPa. The data for the structural battery inventory is mainly based on data found in Harnden et al. (2022), but have then been adapted to represent a CF,CF/LiFePO₄ battery with a cellulose separator. Harnden et al. (2022) report on a structural battery with both electrodes made from CF and a Freudenberg separator, where the average volume fraction of the carbon fibres to the structural battery electrolyte in the electrodes was 49%. Table 1 shows the densities of the carbon fibres and structural battery electrolyte as reported by Harnden et al. (2022).

Table 1: Densities of the materials in the structural battery, based on data from Harnden et al. (2022).

Material	Density (g/cm ³)
Carbon fibre	1.8
Structural battery electrolyte (SBE)	1.23

To be able to obtain the masses of the different materials, we need to know the volumes used. We assume an area of 10*10 cm for the battery. Harnden et al. (2022) assumes an average carbon fibre volume fraction of 49 vol% and the electrolyte volume fraction is 51 vol% in the layers. We assume that the negative electrode layer has a volume fraction of 49% carbon fibres, while the volume fraction of carbon fibres is likely to be lower in the positive electrode due to the carbon fibre coating LiFePO₄ taking up volume. In this study, we assume 37 vol% carbon fibres in the positive layer.

Negative electrode

The CF layers were 32 μm each (positive and negative electrode). In these layers, there are 49 vol% CF and 51vol% SBE, using the densities in Table 1, this means that:

$$\text{Volume carbon negative electrode layer} = 10 \text{ cm} * 10 \text{ cm} * 32 * 10^{-4} \text{ cm} = 0.32 \text{ cm}^3$$

$$\begin{aligned} \text{Volume of carbon fibres in negative electrode layer} &= 0.32 \text{ cm}^3 * 49\text{vol}\% \text{ CF} \\ &= 0.1568 \text{ cm}^3 \end{aligned}$$

$$\begin{aligned} \text{Volume of electrolyte in cnegative electrode layer} &= 0.32 \text{ cm}^3 * 51\text{vol}\% \text{ CF} \\ &= 0.1632 \text{ cm}^3 \end{aligned}$$

The masses are then:

$$\begin{aligned} \text{Mass of carbon fibre in negative electrode layer} &= 0.1568 \text{ cm}^3 * 1.8 \frac{\text{g}}{\text{cm}^3} \\ &= 0.28224\text{g} \end{aligned}$$

$$\begin{aligned} \text{Mass of electrolyte in negative electrode layer} &= 0.1632 \text{ cm}^3 * 1.23 \frac{\text{g}}{\text{cm}^3} \\ &= 0.200736\text{g} \end{aligned}$$

Positive electrode

The CF layers were 32 μm each. In these layers, it is assumed that there are 37 vol% CF. The CFs are coated with LiFePO_4 , which takes up some space. We know that the uncoated fibres have a diameter of 5 μm ($r=2.5 \mu\text{m}$), and that the layer of LiFePO_4 coating is 1 μm thick, meaning that the coated carbon fibres have a diameter of 7 μm . Note that there is a possibility to vary the packing of the LiFePO_4 coating, leading to a higher or lower volume of electrolyte in the positive electrode layer, we have however excluded this from our study.

$$\text{Volume positive electrode} = 10 \text{ cm} * 10 \text{ cm} * 32 * 10^{-4} \text{ cm} = 0.32 \text{ cm}^3$$

$$\begin{aligned} \text{Volume of carbon fibres in positive electrode} &= 0.32 \text{ cm}^3 * 37 \text{ vol\% CF} \\ &= 0.1184 \text{ cm}^3 \end{aligned}$$

We calculate the volume of LiFePO_4 coating needed:

$$\text{Volume fraction LiFePO}_4 \text{ coating in layer} = \frac{V_{\text{LiFePO}_4 \text{ coating}}}{V_{\text{Fiber}}} *$$

$$\text{Volume fraction of CF} = \frac{\pi * (3.5^2 - 2.5^2) * h}{\pi * 2.5^2 * h} * 0.37 = 0.3552$$

$$\begin{aligned} \text{Volume of LiFePO}_4 \text{ coating in positive electrode} \\ &= 0.32 \text{ cm}^3 * 36 \text{ vol\% LiFePO}_4 \text{ coating} = 0.1136 \text{ cm}^3 \end{aligned}$$

This means that the volume of electrolyte in the positive electrode layer is

$$\begin{aligned} \text{Volume of electrolyte in carbon fiber layer} \\ &= 0.32 \text{ cm}^3 * (1 - 37 \text{ vol\% CF} - 36 \text{ vol\% LiFePO}_4 \text{ coating}) = 0.088 \text{ cm}^3 \end{aligned}$$

Johannisson et al. (2019b) writes that the mass ratio needed for coating of the positive electrode is 89:6:5 (LiFePO_4 : Carbon black: Polyvinylidene fluoride). To calculate this into volume relationships, the mass fractions are divided by the densities of the materials. We assume that the density of LiFePO_4 is 3.47 g/cm^3 (Materials Project, n.d.), the density of carbon black is assumed to be 1.95 g/cm^3 (average of what is reported in Flexicon (n.d.)) and the density of polyvinylidene fluoride is assumed to be 1.78 g/mL (cm^3) (Guidechem, n.d.) The resulting volume ratio is then: 25.6:3.1:2.8 which corresponds to 81:10:9 (LiFePO_4 : Carbon black: Polyvinylidene fluoride). This means that 81% of the volume LiFePO_4 coating is LiFePO_4 , 10% is carbon black, and 9% is polyvinylidene fluoride.

This means that the masses for the three components are:

$$\text{Mass of LiFePO}_4 \text{ in positive electrode} = 0.1136 \text{ cm}^3 * 0.81 * \frac{3.47 \text{ g}}{\text{cm}^3} = 0.32 \text{ g}$$

$$\text{Mass of carbon black in positive electrode} = 0.1136 \text{ cm}^3 * 0.10 * \frac{1.95 \text{ g}}{\text{cm}^3} = 0.021 \text{ g}$$

$$\begin{aligned} \text{Mass of polyvinylidene fluoride in positive electrode} &= 0.1136 \text{ cm}^3 * 0.10 * \frac{1.78 \text{ g}}{\text{cm}^3} \\ &= 0.018 \text{ g} \end{aligned}$$

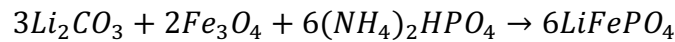
$$\text{Mass of CF in positive electrode} = 0.1184 \text{ cm}^3 * 1.8 \frac{\text{g}}{\text{cm}^3} = 0.21312 \text{ g}$$

$$\text{Mass of electrolyte in positive electrode} = 0.088 \text{ cm}^3 * 1.23 \frac{\text{g}}{\text{cm}^3} = 0.108 \text{ g}$$

In addition to this, Zackrisson et al. (2019) writes that 1 kJ electricity is needed for each gram of coated fiber.

LiFePO₄ production

Data for LiFePO₄ production was taken from Dunn et al. (2015), and the production is assumed to be made by means of solid-state synthesis with the following chemical reaction



Using the stoichiometric relationships, this results in the following masses:

	Molar mass (g)	Mass input (g)	Mass output (g)
• 3Li₂CO₃	73.9	222	
• 2Fe₃O₄	231.5	463	
• 6(NH₄)₂HPO₄	132.1	792	
• 6LiFePO₄	157.8		947

The energy use for producing LiFePO₄ is assumed to be 3 kJ electricity/gram. This includes energy for heating and grinding (Zackrisson et al., 2010).

Cellulose separator

We assume that the cellulose separator is 24 micrometers thick (Lv et al., 2021). The cellulose separator is assumed to have a porosity of 61% (average as reported in (Kim et al., 2018) and that the absolute density is 1.5 g/cm³ (same as cellulose). We also assume that the cellulose maintains the same thickness as when dry after being assembled in the battery cell.

This gives us the numbers:

$$\text{Volume separator layer} = 10 \text{ cm} * 10 \text{ cm} * 24 * 10^{-4} \text{ cm} = 0.24 \text{ cm}^3$$

$$\begin{aligned} \text{Volume of separator in separator layer} &= 0.24 \text{ cm}^3 * (100 - 61) \text{ vol\% separator} \\ &= 0.0936 \text{ cm}^3 \end{aligned}$$

$$\text{Volume of SBE in separator layer} = 0.24 \text{ cm}^3 * 61 \text{ vol\% SBE} = 0.1464 \text{ cm}^3$$

The mass of the separator and the SBE is then

$$\text{Mass of cellulose in separating layer} = 0.0936 \text{ cm}^3 * 1.5 \frac{\text{g}}{\text{cm}^3} = 0.1404 \text{ g}$$

$$\text{Mass of SBE in separating layer} = 0.1464 \text{ cm}^3 * 1.23 \frac{\text{g}}{\text{cm}^3} = 0.180 \text{ g}$$

Current collector

The current collectors are assumed to be 0.01 mm (Johannisson et al., 2021) thick, 8 mm (Tasneem & Siam Siraj, 2022) wide and be required every 100 mm of the structural battery length. This means that the amount of current collector, in reality, will be different for each car part depending on its dimensions. In this assessment, for simplicity, we will use an approximated amount. This amount is based on the mount of current collector on a structural battery of 1 m² with the dimensions 100*100*1 cm.

This means that the fictious battery needs 10 strips of 100 cm long strips. This means that the volume of current collector needed is

$$\begin{aligned} \text{Volume of current collector for } 1\text{m}^2\text{SB} \\ &= 10 \text{ strips} * 100 \text{ cm long} * 0.8 \text{ cm wide} * 0.001 \text{ cm thick} = 0.8 \text{ cm}^3 \\ &= 8 * 10^{-7} \text{ m}^3 \end{aligned}$$

It is assumed that the current collector for the negative electrode is made from copper and that it has the density of 8960 kg/m³ (Royal Society of Chemistry). This means that the mass of the collector for the current collector is:

$$\text{Mass of current collector NE} = 8 * 10^{-7} \text{ m}^3 * \frac{8960 \text{ kg}}{\text{m}^3} = 7.168 * 10^{-3} \text{ kg}$$

The volume of our fictious SB is 0.01 m³, and the density of a generic structural battery is assumed to be 1.69 g/cm³. The mass of our fictious battery is then

$$\text{Mass of fictious SB} = 0.01 \text{ m}^3 * \frac{1690 \text{ kg}}{\text{m}^3} = 16.9 \text{ kg}$$

This means that the approximated amount of current collector per kg of battery is

$$\begin{aligned} \text{kg current collector (NE) per kg SB} &= \frac{7.168 * 10^{-3} \text{ kg current collector}}{16.9 \text{ kg SB}} \\ &= 4.2 * 10^{-4} \text{ g current collector per g SB} \end{aligned}$$

The positive electrode has a current collector made from aluminium. It is assumed that the same volume of current collector is needed as for the copper current collector. The density of aluminum is assumed to be 2.71 g/cm³ (Thyssenkrupp, 2022)

$$\text{Mass of current collector (PE)} = 8 * 10^{-7} \text{ m}^3 * \frac{2710 \text{ kg}}{\text{m}^3} = 2.16 * 10^{-3} \text{ kg}$$

Per kg of Sb, this is then

$$\begin{aligned} \text{kg current collector (PE) per kg SB} &= \frac{2.16 * 10^{-3} \text{ kg current collector}}{16.9 \text{ kg SB}} \\ &= 1.3 * 10^{-4} \text{ g current collector per g SB} \end{aligned}$$

Note that these values are an approximation and will depend on the width, thickness, and specific density of the structural battery in each application.

Casing

The casing is assumed to be produced from 65 vol% carbon fibres and 35 vol% epoxy (density assumed to be 1.15 g/cm³ which is the average value reported by Bhatia et al. (2019)). The size of the casing is based on data found in Zackrisson et al. (2019) target design of a structural battery. They write that the casing will require 8.75 wt% glass fibre and 4.29 wt% epoxy (in relation to total battery mass). In our case, this corresponds to the casing being 10 vol% of the battery cell and 74 wt% CF and 26 wt% epoxy (in relation to the casing alone).

Assembly of the battery

Zackrisson et al. (2019) suggests that battery assembly and lithium cell manufacturing in clean/dry rooms requires 11.7 kwh electricity and 8.8 kwh gas per kg of structural battery.

The resulting mass of the SBC described above is 1.62 g and the volume is 0.97 cm³, which results in a density of 1.68 g/cm³.

Life cycle inventory

Carbon fibre production

The inventory for the carbon fibre production can be found in Table 2.

Table 2: The data for the carbon fibre production, adapted from Romaniw (2013)

	Amount	Unit	Provider
Inputs			
Air	240.0	kg	
electricity, low voltage	116248.6	kJ	market group for electricity, low voltage electricity, low voltage Cutoff, U - RER
nitrogen, liquid	20.75	kg	market for nitrogen, liquid nitrogen, liquid Cutoff, U - RER
Production of PAN fibres	1.718	kg	ELCD dataset by Fazio and Pennington (2005). Adapted to fit Ecoinvent nomenclature (see Hermansson et al. (2022a) for details)
Outputs			
Ammonia	0.076	kg	
Argon	2.4	kg	
Carbon dioxide, fossil	0.305	kg	
Carbon monoxide, fossil	0.054	kg	
Hydrogen	0.021	kg	
Hydrogen cyanide	0.283	kg	
Methane, fossil	0.027	kg	
Nitrogen	208.104	kg	
Oxygen	50.245	kg	
Waste water	0.409	kg	
Carbon fibres	1	kg	

Lignin based carbon fibre production

The lignin is assumed to come from an Organsolv process as described by Moncada et al. (2018). The spinning is assumed to be melt spinning and require 0.1036 kWh electricity¹/kg fibre (Das, 2011). We assume no losses in the spinning phase. The lignin-based carbon fibre production is also based on Romaniw (2013) but is adapted so that there is biogenic emissions of carbon dioxide and carbon monoxide. Also, the methane emissions are assumed to be from soil or biomass stock. Finally, we assume that the carbonization and stabilization of lignin requires 25% less energy than PAN in line with what is suggested by Das (2011). The inventory for the lignin-based carbon fibre production can be found in Tables 3 and 4.

¹ Using the provider "market group for electricity, low voltage | electricity, low voltage | Cutoff, U – RER"

Table 3: Inventory for the lignin production, adapted from Hermansson et al. (2022b) and based on Moncada et al. (2018).

Flow	Amount	Unit	Provider
Inputs			
cooling energy	998.0	TJ	market for cooling energy cooling energy Cutoff, U - GLO
electricity, low voltage	13.0	TJ	market group for electricity, low voltage electricity, low voltage Cutoff, U - RER
enzymes	1.0*10 ⁷	kg	market for enzymes enzymes Cutoff, U - GLO
Solvent	10000.0	kg	market for ethanol, without water, in 99.7% solution state, from fermentation ethanol, without water, in 99.7% solution state, from fermentation Cutoff, U - GLO
heat, district or industrial, natural gas	1375.0	TJ	market group for heat, district or industrial, natural gas heat, district or industrial, natural gas Cutoff, U - RER
sulfuric acid	6000000.0	kg	market for sulfuric acid sulfuric acid Cutoff, U - RER
tap water	4.231*10 ⁹	kg	market group for tap water tap water Cutoff, U - RER
wood chips, wet, measured as dry mass	1.111*10 ⁹	kg	market for wood chips, wet, measured as dry mass wood chips, wet, measured as dry mass Cutoff, U - Europe without Switzerland
Outputs			
Carbon dioxide, biogenic	1000000.0	kg	
Chemically polluted water	2.989*10 ⁹	kg	
Furfural	1.2*10 ⁷	kg	
Hemicellulosic sugars	9.5*10 ⁸	kg	
C6 sugars	3.59*10 ⁸	kg	
Organosolv lignin	1.91*10 ⁸	kg	
Waste, unspecified	8.57*10 ⁸	kg	

In this study, we use mass allocation. The three products of the system are: furfural, C6 sugars and lignin. This results in the mass allocation factor 0.34 for lignin, as calculated below.

$$\begin{aligned}
 \text{Total mass output} &= \text{Mass}_{C6 \text{ sugars}} + \text{Mass}_{Furfural} + \text{Mass}_{lignin} \\
 &= 3.59 * 10^8 \text{ kg} + 1.2 * 10^7 \text{ kg} + 1.91 * 10^8 \text{ kg} = 5.62 * 10^8 \text{ kg}
 \end{aligned}$$

The mass allocation factor for lignin is then:

$$\text{Mass allocation factor}_{lignin} = \frac{1.91 * 10^8}{5.62 * 10^8} = 0.34$$

Table 4: The production of lignin based carbon fibres, adapted and based on data from Romaniw (2013) combined with Das (2011)

Flow	Amount	Unit	Provider
Inputs			
Air	240.0	kg	
electricity, low voltage	87186.45	kJ	market group for electricity, low voltage electricity, low voltage Cutoff, U - RER
Lignin based precursor fiber spinning	1.718	kg	Lignin based precursor fiber spinning (See text above)
nitrogen, liquid	20.75	kg	market for nitrogen, liquid nitrogen, liquid Cutoff, U - RER
Outputs			
Ammonia*	0.076	kg	
Argon	2.4	kg	
Carbon dioxide, biogenic	0.305	kg	
Carbon monoxide, biogenic	0.054	kg	
Hydrogen	0.021	kg	
Hydrogen cyanide	0.283	kg	
Methane, from soil or biomass stock	0.027	kg	
Nitrogen	208.104	kg	
Oxygen	50.245	kg	
Waste water	0.409	kg	
Lignin-based carbon fibres	1.0	kg	

*Included even though it is likely that ammonium is emitted exclusively during the carbonization of PAN due to embedded nitrogen. However it is included due to uncertainties.

When assessing the influence of microwave technology the energy used in the PAN-based carbon fibre production was multiplied with 0.0653 (in line with average value in Lam et al. (2019)) to generate the energy consumption when using microwave technology. In the bioeconomy scenario, the energy use for lignin carbon fibre production was multiplied with the same number.

LiFePO₄ production

The inventory for the LiFePO₄ production can be found in Table 5 and is described earlier in this document.

Table 5: The inventory for the LiFePO₄ production

Flow	Amount	Unit	Provider
Inputs			
<i>Li₂CO₃</i>	0.23	g	market for lithium carbonate lithium carbonate Cutoff, U - GLO
<i>Fe₃O₄</i>	0.49	g	market for magnetite magnetite Cutoff, U
<i>(NH₄)₂HPO₄</i>	0.84	g	diammonium phosphate production diammonium phosphate Cutoff, U - RER
<i>Electricity</i>	3	kJ	market group for electricity, low voltage electricity, low voltage Cutoff, U - GLO
Outputs			
<i>LiFePO₄</i>	1	g	

Production of Structural battery electrolyte

The production of the structural battery electrolyte was based on data collected in the lab, and from Tasneem and Siam Siraj (2022) and is found in Table 6. The recipe for the electrolyte production is 0.1 g initiator, 5g liquid electrolyte, and 5 g monomer. The mass composition for the liquid electrolyte is 6.5:6.5:0.94:0.78 (ethylene carbonate: propylene carbonate: Lithium trifluoromethanesulfonate: Lithium bis(oxalato)borate)

Table 6: The composition of the structural battery electrolyte, based on (Tasneem & Siam Siraj, 2022) and data from the lab.

		Mass (g)	Process in ecoinvent	Density (approximations)
Inputs				
Polymer	Bisphenol A dimethacrylate	5	market for bisphenol A, powder bisphenol A, powder Cutoff, U - GLO	1.12 g/cm ³ (Sigma-Aldrich, n.d.-b)
	2,2'-Azobis(2-methylpropionitrile)	0.1	market for chemical, organic chemical, organic Cutoff, U - GLO	0.858 g/cm ³ (Sigma-Aldrich, n.d.-a)
Liquid electrolyte	Lithium trifluoromethanesulfonate	0.32	market for chemical, inorganic chemical, inorganic Cutoff, U ²	1.88 g/cm ³ (Stanford Advanced Materials, n.d.)
	Ethylene carbonate	2.2	market for ethylene carbonate ethylene carbonate Cutoff, U-GLO	1.32 g/cm ³ (ChemBK, n.d.)
	Propylene carbonate	2.2	market for chemical, organic chemical, organic Cutoff, U - GLO	1.20 g/cm ³ (Sigma-Aldrich, n.d.-c)
	Lithium bis(oxalato)borate	0.27	market for chemical, inorganic chemical, inorganic Cutoff, U-GLO	1.78 g/cm ³ (Albemarle, 2018)
Outputs				
	Structural battery electrolyte		10.1	1.23 (Harnden et al., 2022).

The volume fractions of the liquid electrolyte and polymer matrix were calculated using the values above but needed to be adapted to fit the total volume of the electrolyte in the SBC that was calculated using volume fractions on a layer basis (as the densities vary depending on producer and form of chemical). This was done by calculating the vol% of the liquid electrolyte and polymer matrix using the densities above to get a distribution between the two phases, then multiplying these volumes with the total volume of electrolyte that was calculated for the structural battery composite layers.

² Approximation as this is a salt, however also containing carbon

Structural battery composite manufacturing

The inventory for the SBC manufacturing can be found in Table 7.

Table 7: The inventory for production of 1.6 g of structural battery composite

Structural battery composite part	Amount	Flow	Provider
Inputs			
Positive electrode	Carbon fibre (g)	0.21	See Tables 3 and 4
	LiFePO4 (g)	0.32	See Table 5
	Polyvinylidene Fluoride (g)	0.018	market for polyvinylfluoride, dispersion polyvinylfluoride, dispersion Cutoff, U – GLO ³
	Carbon black (g)	0.022	market for carbon black carbon black Cutoff, U – GLO
	Electricity (kJ)	0.21	market group for electricity, low voltage electricity, low voltage Cutoff, U – RER
Negative electrode	Carbon fibre (g)	0.28	See Tables 3 and 4
Electrolyte	Polymer matrix (g)	0.25	See Table 5
	Liquid electrolyte (g)	0.24	See Table 5
Separator	Cellulose fabric (g)	0.14	tissue paper production, virgin tissue paper Cutoff, U – GLO
Current collectors	Aluminium (g)	$1.9 \cdot 10^{-4}$	Li-ion battery aluminium collector foil, for Li-ion battery Cutoff, U - GLO
	Copper (g)	$6.3 \cdot 10^{-4}$	market for copper collector foil, for Li-ion battery copper collector foil, for Li-ion battery Cutoff, U – GLO
Casing	Epoxy (g)	0.035	market for epoxy resin, liquid epoxy resin, liquid Cutoff, U – RER
	Carbon fibre (g)	0.10	See Tables 3 and 4
Manufacturing	Electricity (kwh)	0.019	market group for electricity, low voltage electricity, low voltage Cutoff, U – RER
	Gas (kwh)	0.014	market group for heat, district or industrial, natural gas heat, district or industrial, natural gas Cutoff, U – RER
Outputs			
Structural battery composite (g)		1.6	n/a

³ Approximation as Polyvinylidene fluoride is lacking in Ecoinvent

Note that all electricity in production and manufacturing in the foreground system is assumed to come from low-voltage electricity. This is because of the usually small production facilities connected to the materials used, but also because of the types of materials not needing the same voltage as, for example, metals. The results using medium voltage electricity, which would be the other choice depending on size and equipment is assumed to be slightly smaller, with a difference on the verge to neglectable to the results using low-voltage electricity.

Conventional vehicle manufacturing

The inventory for the manufacturing of the metal car parts is found in Tables 8 and 9. It is assumed that the material efficiency in the shaping (deep drawing) of the aluminium car parts manufacturing is 57.5% and 65% for steel. The waste metals are assumed to be sent to a recycling facility. In the metal car part base case, the cut-off approach is applied to handle the partitioning of steel scrap between life cycles.

Table 8: The inventory for production of aluminium car parts

Flow	Amount	Unit	Provider
Inputs			
Aluminium, primary, ingot	1.74	kg	market for aluminium, primary, ingot aluminium, primary, ingot Cutoff, U - IAI Area, EU27 & EFTA
Sheet rolling, aluminium	1.74	kg	sheet rolling, aluminium sheet rolling, aluminium Cutoff, U - RER
Deep drawing aluminium	1.74	kg	deep drawing, steel, 650 kN press, automode deep drawing, steel, 650 kN press, automode Cutoff, U - RER (Proxy due to data availability)
Outputs			
Aluminium car parts	1.0	kg	n/a
Aluminium waste	0.74	kg	market for aluminium, primary, ingot aluminium, primary, ingot Cutoff, U - IAI Area, EU27 & EFTA

Table 9: The inventory for production of steel car parts

Flow	Amount	Unit	Provider
Inputs			
Steel, low-alloyed	1.54	kg	steel production, converter, low-alloyed steel, low-alloyed Cutoff, U - RER
Sheet rolling, steel	1.54	kg	sheet rolling, steel sheet rolling, steel Cutoff, U - RER
Deep drawing steel	1.54	kg	deep drawing, steel, 650 kN press, automode deep drawing, steel, 650 kN press, automode Cutoff, U - RER
Outputs			
Steel car part	1.0	kg	n/a
Steel waste	0.54	kg	steel production, converter, low-alloyed steel, low-alloyed Cutoff, U - RER

In the case where we include the use of recycled metals in the assessment, we assume that the scrap that is created in the car part manufacturing is recycled into the same system in a closed loop. The use of recycled metals is then credited the system for replacing inputs of primary materials (this is when using the cut-off allocation approach).

The credits are 0.74 kg for aluminium and 0.54 kg for steel, meaning that the input of aluminium and steel in this case is 1 kg each.

Mass of car parts

In our study, we include a roof and the doors of the vehicle made from steel and the hood made from aluminium, the specifications for the materials are found in Table 10.

Table 10: The specifics for the metal car parts

	Roof	Hood	Doors	Reference
Material	Steel	Aluminium	Steel	
Number	1	1	4	
Density (kg/m ³)	7850	2710	7850	(Eurocode, n.d.) and (Thyssenkrupp, 2022)
Effective modulus (GPa)	210	78.25 ⁴	210	(AZO Materials, n.d.) and (Eurocode, n.d.)
Specific modulus (GPa/kg/m ³)	0.027	0.029	0.027	
Length (m)	2.2	1.7	0.8	
Width (m)	1.1	1.2	1.1	
Thickness (m)	0.0008	0.0009	0.0007	
Total volume (m ³)	0.0019	0.0018	0.0025	
Mass (kg)	15.2	4.98	19.3	

It is assumed that the corresponding structural battery composite car parts needs to have the same flexural stiffness as the conventional car parts. The flexural stiffness in turns influences how thick the structural composite car parts needs to be.

This means that

$$E_{Conv} * I_{Conv} = E_{SB} * I_{SB}$$

Where E is the effective and I is the moment of inertia

$$I = \frac{1}{3} * width * thickness^3$$

The thickness of the structural composite car parts (all assumed to be rectangular/square) is calculated using the following equation:

$$thickness_{SB} = \sqrt[3]{\frac{thickness_{conv}^3 * Effective\ modulus_{Conv}}{Effective\ modulus_{SB}}}$$

⁴ Average of maximum 88.5 GPa and minimum 68 GPa

The resulting thicknesses and volumes for the SB parts are found in Table 11.

Table 11: The specifics for the SBC car parts

	Roof	Hood	Doors
Material	Structural battery composites	Structural battery composites	Structural battery composites
Number	1	1	4
Density (kg/m ³)	1678	1678	1678
Effective modulus (GPa)	70	70	70
Specific modulus (GPa/kg/m ³)	0.042	0.042	0.042
Length (m)	2.2	1.7	0.8
Width (m)	1.1	1.2	1.1
Thickness (m)	0.00115	0.000934	0.00101
Total volume (m ³)	0.00279	0.00191	0.00355
Total mass (kg)	4.68	3.20	5.96

Lightweighting and avoided Li-ion battery production

The total lightweighting of the vehicle is calculated using the following equations:

$$\Delta m_{SBC\ vehicle} = \Delta m_{Li-ion\ battery} + \Delta m_{material}$$

Where the Li-ion battery avoided production is calculated by

$$Energy\ storage_{SBC} = Energy\ density_{SBC} \left(\frac{Wh}{kg} \right) * m_{SBC} (kg) = Wh\ in\ SBC\ car\ parts$$

$$\begin{aligned} \Delta m_{Li-ion\ battery} &= \frac{Energy\ storage_{SBC} (Wh)}{Energy\ density_{Li-ion\ battery} \left(\frac{Wh}{kg} \right)} \\ &= kg\ Li - ion\ battery\ that\ is\ replaced \end{aligned}$$

The credit from vehicle weight reduction is calculated by:

$$\begin{aligned} &Energy\ saved\ during\ use\ phase \\ &= \Delta m_{SBC\ vehicle} * Fuel\ reduction\ value * Distance\ driven \end{aligned}$$

Where Δm is the difference in mass of the vehicle due to the exchange of the conventional part to the structural battery. Note that this value also includes the decrease in mass due to a smaller battery and that the SBC vehicle also is given a credit for avoided production of the li-ion battery.

The fuel reduction value for the vehicle is assumed to be 0.069 Wh/kg/km Forell et al. (2016) as cited in Johannisson et al. (2019a). In this study, the base case distance is set to 200 000 km.

The weight reduction is presented in Table 12.

Table 12: The weight reduction when switching from metals to SBC

	Conventional vehicle	Structural battery composite vehicle
Material	Aluminium and steel	Structural battery composites
kg	4.98 kg aluminium parts 34.54 kg steel parts	13.84 (15.23 including losses in manufacturing)
$\Delta m_{battery}$ (kg)	6.78	
$\Delta m_{SBC\ vehicle}$	32.45	
Reduced fuel use in use phase (kWh)	447.8	

To model the avoided fuel use in the use phase, we used the process “market group for electricity, low voltage | electricity, low voltage | Cutoff, U – RER” and for avoided battery production “market for battery, Li-ion, NMC111, rechargeable, prismatic | battery, Li-ion, NMC111, rechargeable, prismatic | Cutoff, U – GLO”.

End of life treatment

The SBC material being wasted in the SBC manufacturing (1.38 kg) is assumed to be sent to landfill, and the process using the process “market for inert waste, for final disposal | inert waste, for final disposal | Cutoff, U – CH”.

To model the end-of-life treatment for the SBC in the vehicle, the following processes listed in Table 13 were used.

Table 13: The processes used to model the waste *) case specific amounts depending on material composition, battery size, and recycling rate

	Amount*	Unit	Provider
Fossil parts of structural battery composite	1	kg	treatment of hazardous waste, hazardous waste incineration hazardous waste, for incineration Cutoff, U SBC - Europe without Switzerland
Bio-based parts of the structural battery composites (separator and lignin-based carbon fibers)	1	kg	treatment of hazardous waste, hazardous waste incineration hazardous waste, for incineration Cutoff- Europe without Switzerland, where the fossil carbon dioxide and carbon monoxide emissions were removed
Li-ion battery	1	kg	market for hazardous waste, for underground deposit hazardous waste, for underground deposit Cutoff, U - RER

When the SBCs are recycled, we assume that the method used is pyrolysis and that the energy carrier is electricity using the provider “market group for electricity, low voltage | electricity, low voltage | Cutoff, U – RER”

For the conventional vehicles metal car parts not having a second life, the processes “market for scrap aluminium | scrap aluminium | Cutoff, U - Europe without Switzerland” and “treatment of scrap steel, inert material landfill | scrap steel | Cutoff, U – CH” are used.

Cradle-to-gate results

Figure 1 shows the distribution of climate impact and energy use for manufacturing 1 kg of SBC. Figure 2 shows the terrestrial acidification, metal depletion, ozone depletion, and water depletion for the manufacturing of 1 kg SBC using ReCiPe midpoint (H).

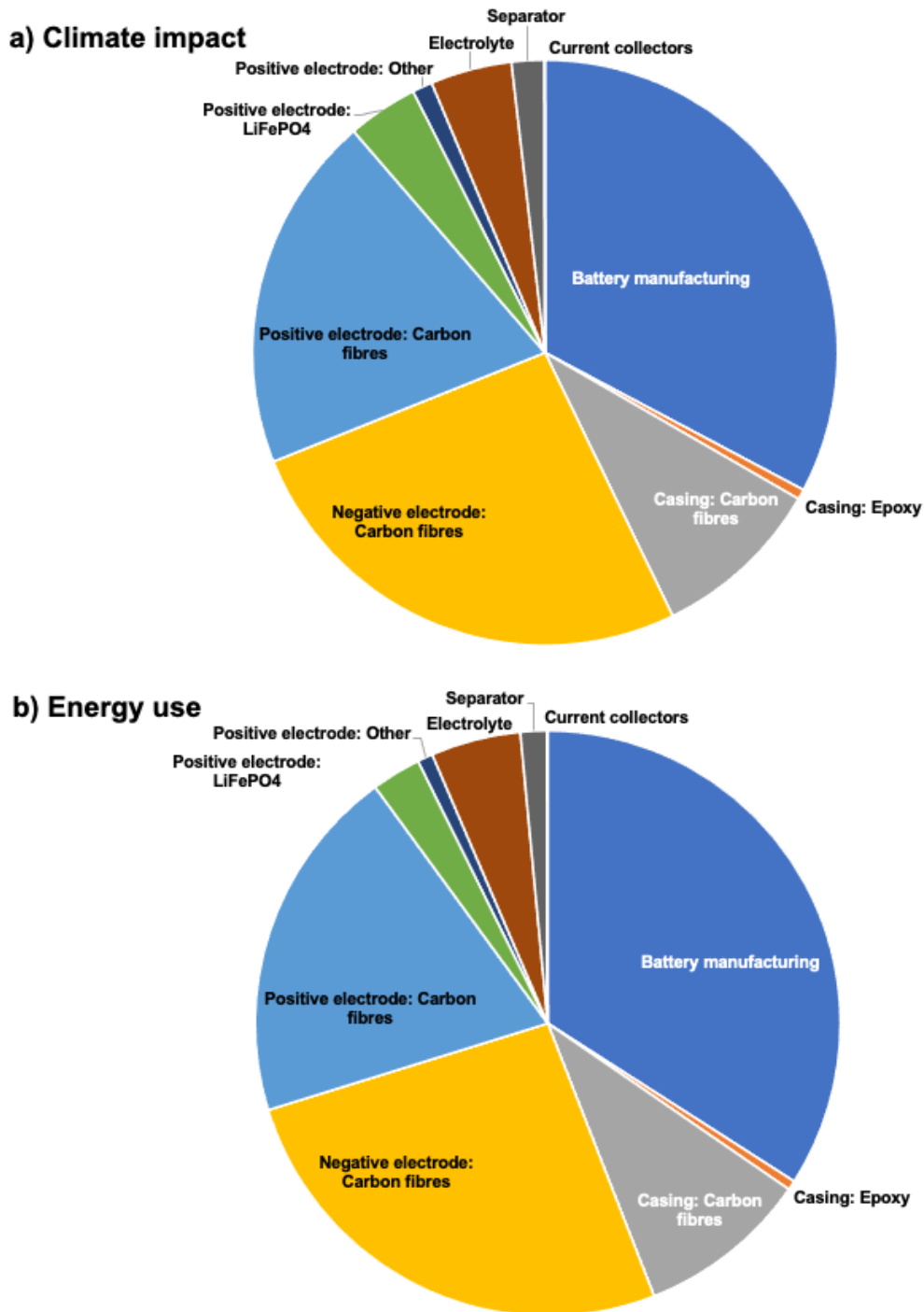


Figure 1: The distribution of a) climates impact and b) energy consumption for the production of 1 kg of structural battery composites.

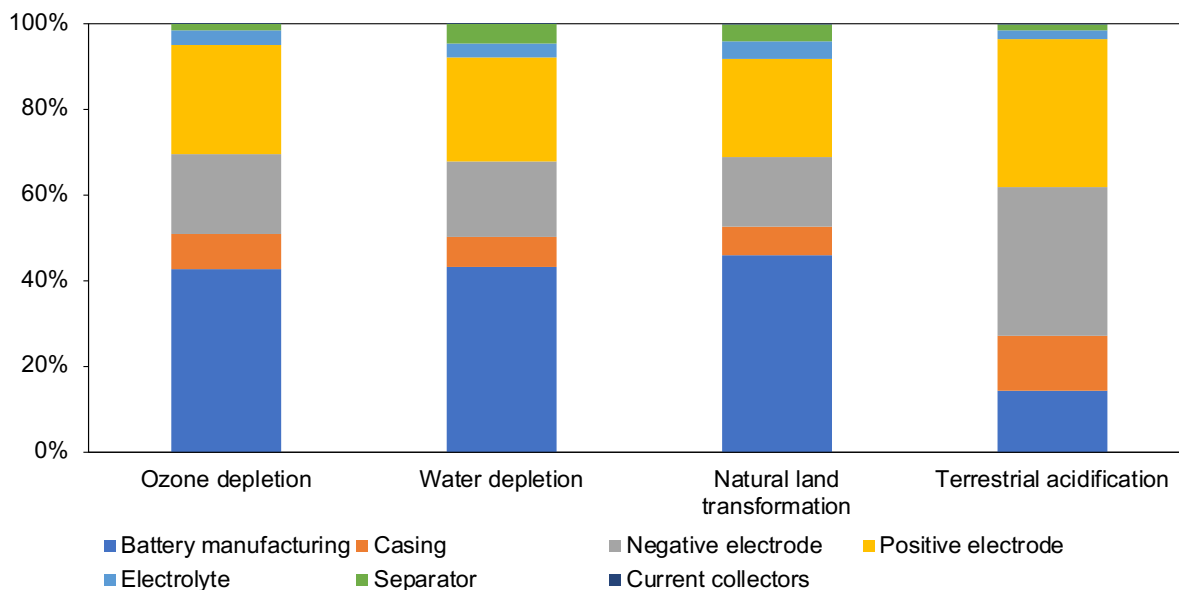


Figure 2: Normalized midpoint results for the manufacturing of 1 kg of structural battery composites.

Figure 2 shows similar results as for climate impact and energy use, where the energy for manufacturing is a main contributor. The largest deviation is for terrestrial acidification, where the emission of ammonia to air in the carbon fibre production process has a large influence.

Sensitivity analysis

The influence of effective modulus, energy density, milage, and energy consumption in the manufacturing phase was varied with 10% up and down. The resulting values are presented in Table 14.

Table 14: Values used in the sensitivity analysis. Note that the sensitivity analysis also changes amounts sent to waste treatment, which is not shown in.

	Base case	Increase in effective modulus	Decrease in effective modulus	Increase in energy density	Decrease in energy density	Increase in milage	Decrease in milage	Increase in energy use	Decrease in energy use	Increase energy reduction value	Decrease in energy reduction value
Effective modulus (GPa)	70	77	63	70	70	70	70	70	70	70	70
Mass of SBC needed (kg) (including losses)	13.8 (15.2)	13.4 (14.8)	14.3 (15.8)	13.8 (15.2)	13.8 (15.2)	13.8 (15.2)	13.8 (15.2)	13.8 (15.2)	13.8 (15.2)	13.8 (15.2)	13.8 (15.2)
Energy density (Wh)	70	70	70	77	63	70	70	70	70	70	70
Avoided Li-ion battery (kg)	6.78	6.57	7.2	7.5	6.1	6.78	6.78	6.78	6.78	6.78	6.78
Recovered Li-ion battery((kg) (only for end-of-life recycling)	2.71	2.62	2.81	2.98	2.44	2.71	2.71	2.71	2.71	2.71	2.71

(Continued)

	Base case	Increase in effective modulus	Decrease in effective modulus	Increase in energy density	Decrease in energy density	Increase in milage	Decrease in milage	Increase in energy use	Decrease in energy use	Increase energy reduction value	Decrease in energy reduction value
Total mass savings (kg)	32.4	32.67	32.2	33.1	31.8	32.4	32.4	32.4	32.4	32.4	32.4
Energy reduction value (Wh/kg/km)	0.069	0.069	0.069	0.069	0.069	0.069	0.069	0.069	0.069	0.076	0.062
Milage (km)	200 000	200 000	200 000	200 000	200 000	220 000	180 000	200 000	200 000	200 000	200 000
Energy saved in use phase (kWh)	447.8	450.8	444.3	457.1	438.4	492.6	403.0	447.8	447.8	492.6	403.0
Energy consumption in use phase (kWh/kg SBC)	Electricity: 11.7 Heat: 8.8	Electricity: 11.7 Heat: 8.8	Electricity: 11.7 Heat: 8.8	Electricity: 11.7 Heat: 8.8	Electricity: 11.7 Heat: 8.8	Electricity: 11.7 Heat: 8.8	Electricity: 11.7 Heat: 8.8	Electricity: 12.9 Heat: 9.7	Electricity: 10.5 Heat: 7.9	Electricity: 11.7 Heat: 8.8	Electricity: 11.7 Heat: 8.8

Decreasing the use of cables

We assume that a NMC111 battery is being replaced by SBCs. The NMC battery has a gross pack energy of 23.5 kWh. The SBC in our base case vehicle has a total energy storage of:

$$\text{Energy capacity of SBC} = \frac{70 \text{ Wh}}{\text{kg SBC}} * 13.84 \text{ kg SBC} = 968.8 \text{ Wh} = 0.97 \text{ kWh}$$

This is approximately 4% of the total Li-ion gross pack energy. We assume that the need of electrical wires is proportional to the gross pack energy, meaning that we can replace 4% of the electrical vehicles electrical wires as we distribute the energy storage in the vehicle. A modern vehicle can have 4 km of electrical wires (Auzanneau, 2013). This means that we could reduce the length of wires by 160 meters.

Different electrical wires will have different compositions and thickness, thus different environmental impacts. If we assume that the wires being replaced are equivalent to “data cables in infrastructure” and using the process “cable production, data cable in infrastructure | cable, data cable in infrastructure | Cutoff, U – GLO” this could offset 41 kg CO₂ eq. and 896 MJ eq throughout the vehicle’s life cycle. In addition to this, the vehicle would also be lighter, thus saving even more fuel in the use-phase. The cables in the dataset used weight on average 0.0545 kg/m, meaning that an additional 120 kWh could be saved throughout the lifecycle.

Changing energy mix

Changing the energy mix using OpenLCA and Ecoinvent is not straight forward. It needs to be done manually for each energy flow. This means that the change cannot be done in a completely consistent way and that the results should be seen as an indication of a possible impact from using a different energy mix. As a general rule, we only changed processes contributing to more than 10% of the total climate impact. We also changed the electricity supplier to a Swedish electricity supplier and natural gas was changed to “heat and power co-generation, natural gas, conventional power plant, 100MW electrical | heat, district or industrial, natural gas | Cutoff, U – SE” and all other energy flows such as oil etc. to “heat, from municipal waste incineration to generic market for heat district or industrial, other than natural gas | heat, district or industrial, other than natural gas | Cutoff, U – SE” to mimic a future carbon lean energy system. Steam use was not changed, except for in the enzyme production used in the Organosolv process and all transportation was left unchanged. Below follows a description on how the different datasets were changed.

Traditional BEV

Steel

We adjusted the process “steel production, converter, low-alloyed | steel, low-alloyed | Cutoff, U - RER” where the electricity supplier was changed to Swedish and the use of natural gas was changed to “market for natural gas, high pressure | natural gas, high pressure | Cutoff, U – SE”.

The process “market group for heat, district or industrial, other than natural gas | heat, district or industrial, other than natural gas | Cutoff, U – RER” was changed to “heat, from municipal waste incineration to generic market for heat district or industrial, other than natural gas | heat, district or industrial, other than natural gas | Cutoff, U – SE”, the process “market group for heat, district or industrial, natural gas | heat, district or industrial, natural gas | Cutoff, U – RER” was changed to “heat and power co-generation, natural gas, conventional power plant, 100MW electrical | heat, district or industrial, natural gas | Cutoff, U – SE”, and the electricity was changed to a Swedish supplier. Finally, the electricity use in the process “deep drawing, steel, 650 kN press, automode | deep drawing, steel, 650 kN press, automode | Cutoff, U – RER” was changed to a Swedish provider.

Nitrogen

The process “air separation, cryogenic | nitrogen, liquid | Cutoff, U – RER” was updated in terms of electricity supplier being Swedish.

Aluminium

For the process “market for aluminium, primary, ingot | aluminium, primary, ingot | Cutoff, U IAI area EU27 och EFTA” all aluminium inputs were changed to the process “aluminium production, primary, ingot | aluminium, primary, ingot | Cutoff, U - IAI Area, EU27 & EFTA” which was altered as described as follows: The electricity provider was changed to be a Swedish and heat was assumed to come from “heat and power co-generation, natural gas, conventional power plant, 100MW electrical | heat, district or industrial, natural gas | Cutoff, U – SE” and “heat, from municipal waste incineration to generic market for heat district or industrial, other than natural gas | heat, district or industrial, other than natural gas | Cutoff, U – SE”. The nitrogen production was altered as previously described in this section. The input “aluminium production, primary, liquid, prebake | aluminium, primary, liquid | Cutoff, U - IAI Area, EU27 & EFTA” was updated to have a Swedish electricity provider. Finally, the market provider of aluminium oxide, metallurgical was assumed to only have the provider “aluminium oxide production | aluminium oxide, metallurgical | Cutoff, U - IAI Area, EU27 & EFTA”, which was updated to only have Swedish electricity providers and heat from “heat and power co-generation, natural gas, conventional power plant, 100MW electrical | heat, district or industrial, natural gas | Cutoff, U – SE”.

Finally, the process “sheet rolling, aluminium | sheet rolling, aluminium | Cutoff, U – RER” was updated to have a Swedish electricity provider and heat inputs from “heat and power co-generation, natural gas, conventional power plant, 100MW electrical | heat, district or industrial, natural gas | Cutoff, U – SE” and “heat, from municipal waste incineration to generic market for heat district or industrial, other than natural gas | heat, district or industrial, other than natural gas | Cutoff, U – SE” and the electricity use in the process “deep drawing, steel, 650 kN press, automode | deep drawing, steel, 650 kN press, automode | Cutoff, U – RER” was changed to a Swedish provider.

Structural battery composites vehicles

PAN-production

The PAN-dataset was updated as described in Hermansson et al. (2022b).

Lignin production

The energy input in the Organosolv process was changed to a Swedish electricity mix and the heat was provided by “heat and power co-generation, natural gas, conventional power plant, 100MW electrical | heat, district or industrial, natural gas | Cutoff, U – SE”.

The energy input in the enzyme production was changed to have a Swedish electricity provider and the flow “Steam in chemical industry” in enzyme assumed to be heat using the process “heat and power co-generation, biogas, gas engine | heat, central or small-scale, other than natural gas | Cutoff, U – SE”.

The electricity used in carbonization and spinning was switched to the Swedish supplier and the nitrogen was changed as described in this section.

LiFePO₄

The process “market for lithium carbonate | lithium carbonate | Cutoff, U -GLO” was changed where the electricity in “lithium carbonate production, from concentrated brine | lithium carbonate | Cutoff, U – GLO” was changed to a Swedish provider. The processes “lithium carbonate production, from spodumene | lithium carbonate | Cutoff, U – RoW”, “lithium carbonate production, from concentrated brine | lithium carbonate | Cutoff, U – GLO” and “lithium carbonate production, from spodumene | lithium carbonate | Cutoff, U – CN” were changed was changed to have a Swedish electricity supplier and heat from “heat and power co-generation, natural gas, conventional power plant, 100MW electrical | heat, district or industrial, natural gas | Cutoff, U – SE”.

Diammonium

The process “diammonium phosphate production | diammonium phosphate | Cutoff, U – RER” was updated where the electricity was changed to a Swedish provider and the heat input was changed to “heat and power co-generation, natural gas, conventional power plant, 100MW electrical | heat, district or industrial, natural gas | Cutoff, U – SE”.

Li-ion battery

The process “market for battery, Li-ion, NMC111, rechargeable, prismatic | battery, Li-ion, NMC111, rechargeable, prismatic | Cutoff, U-GLO” consists of suppliers from CN (China) and RoW (rest of the world), these were updated in the same manner which is described below.

The processes “battery production, Li-ion, NMC111, rechargeable, prismatic | battery, Li-ion, NMC111, rechargeable, prismatic | Cutoff, U” and “battery cell production, Li-ion, NMC111 | battery cell, Li-ion, NMC111 | Cutoff, U” were changed to having Swedish electricity suppliers, tap water from Europe and heat from “heat and power co-generation, natural gas, conventional power plant, 100MW electrical | heat, district or industrial, natural gas | Cutoff, U – SE”.

The process “market for cathode, NMC111, for Li-ion battery | cathode, NMC111, for Li-ion battery | Cutoff, U” were changed where the input “cathode production, NMC111, for Li-ion battery | cathode, NMC111, for Li-ion battery | Cutoff, U ” were updated in terms of electricity supplier to Swedish and heat from “heat and power co-generation, natural gas, conventional power plant, 100MW electrical | heat, district or

industrial, natural gas | Cutoff, U – SE”. The processes for “market for NMC111 oxide | NMC111 oxide | Cutoff, U ” were updated where the inputs from “NMC111 oxide production, for Li-ion battery | NMC111 oxide | Cutoff, U ” were updated where the heat was assumed to be from “heat and power co-generation, natural gas, conventional power plant, 100MW electrical | heat, district or industrial, natural gas | Cutoff, U – SE”.

The process “market for cobalt sulfate | cobalt sulfate | Cutoff, U” was updated in terms of “cobalt sulfate production | cobalt sulfate | Cutoff, U” for the different regions, where the electricity flows were changed to Swedish supplier and heat to “heat and power co-generation, natural gas, conventional power plant, 100MW electrical | heat, district or industrial, natural gas | Cutoff, U – SE”. The process “cobalt production | cobalt hydroxide | Cutoff, U” were assumed to have heat from “heat and power co-generation, natural gas, conventional power plant, 100MW electrical | heat, district or industrial, natural gas | Cutoff, U – SE” and heat from “heat, from municipal waste incineration to generic market for heat district or industrial, other than natural gas | heat, district or industrial, other than natural gas | Cutoff, U – SE” and the process “market for electricity, medium voltage, cobalt industry | electricity, medium voltage, cobalt industry | Cutoff, U – GLO” was changed to “market for electricity, medium voltage | electricity, medium voltage | Cutoff, U – SE”.

Use phase

The electricity provider was changed to “market for electricity, low voltage | electricity, low voltage | Cutoff, U – SE”.

Incineration

The process “treatment of hazardous waste, hazardous waste incineration | hazardous waste, for incineration | Cutoff, U – Europe without Switzerland” was updated in terms of heat where the processes “heat and power co-generation, biogas, gas engine | heat, central or small-scale, other than natural gas | Cutoff, U – SE” (heat, central or small-scale, other than natural gas) and “heat and power co-generation, natural gas, conventional power plant, 100MW electrical | heat, district or industrial, natural gas | Cutoff, U – SE” (heat, district or industrial, natural gas) were used instead of the original suppliers.

Pyrolysis

The electricity consumption in pyrolysis of the structural battery composites when being recycled is switched to the provider “market for electricity, low voltage | electricity, low voltage | Cutoff, U – SE”

Note that this method of transitioning to a carbon lean energy system is not consistent as not all processes and flows could be updated. Likewise, the PAN-dataset consists of elementary flows where the oil resource use was left unchanged as this is a raw material for the PAN-production. It is likely that some share of this is also related to the energy consumption, thus there is some double counting of energy use for this process. For a more in-depth discussion on this, see the supplementary material for Hermansson et al. (2022b).

Net cradle-to-grave results

While the main article focuses on climate impact and energy use, net results for ozone depletion, water use, natural land transformation, and terrestrial acidification was also assessed (using ReCiPe Midpoint (H)). The results are found in Tables 15 and 16.

Table 15: Net impact values for the cradle-to-grave life cycle of the battery electric vehicle for the different technology development routes.

Cut off				
Case	Ozone depletion (kg CFC-11-eq.)	Water depletion (m3)	Natural land transformation (m2)	Terrestrial acidification (kg SO2 eq.)
Conventional vehicle	1.3E-05	1.5E+00	4.0E-02	9.6E-01
Conventional vehicle - recycled materials input	1.2E-05	1.3E+00	3.0E-02	6.3E-01
Conventional vehicle - carbon lean energy	1.2E-05	1.5E+00	3.2E-02	6.4E-01
SBC vehicle - Base case	-1.4E-07	-1.1E+00	-1.9E-02	3.4E-01
SBC vehicle - Biobased fibres	-2.0E-06	-5.3E-01	-2.0E-02	1.1E-01
SBC vehicle - Microwave heating	-3.0E-06	-1.5E+00	-2.6E-02	5.0E-02
SBC vehicle - Recycling	-3.6E-06	-1.2E+00	-2.2E-02	3.0E-01
SBC vehicle - Carbon lean energy	-3.4E-06	-1.1E+00	-2.4E-02	4.0E-01
End-of-life recycling				
Case	Ozone depletion (kg CFC-11-eq.)	Water depletion (m3)	Natural land transformation (m2)	Terrestrial acidification (kg SO2 eq.)
Conventional vehicle	3.2E-06	1.0E+00	1.6E-02	1.5E-01
Conventional vehicle - recycled materials input	3.2E-06	1.0E+00	1.6E-02	1.5E-01
Conventional vehicle - carbon lean energy	2.6E-06	1.0E+00	1.5E-02	1.2E-01
SBC vehicle - Base case	4.3E-06	-6.3E-01	-5.9E-03	8.0E-01
SBC vehicle - Biobased fibres	2.4E-06	-8.5E-02	-6.6E-03	5.7E-01
SBC vehicle - Microwave heating	1.4E-06	-1.0E+00	-1.3E-02	5.2E-01
SBC vehicle - Recycling	-4.0E-06	-7.2E-01	-1.7E-02	-2.2E-01
SBC vehicle - Carbon lean energy	6.4E-07	-6.2E-01	-1.2E-02	8.5E-01

Table 16: Net impact values for the cradle-to-grave life cycle of the battery electric vehicle for the different future scenarios.

Scenarios	Ozone depletion (kg CFC-11-eq.)	Water depletion (m3)	Natural land transformation (m2)	Terrestrial acidification (kg SO2 eq.)
Bioeconomy - Conventional vehicle	1.2E-05	1.5E+00	3.2E-02	6.4E-01
Bioeconomy SBC vehicle	-5.1E-06	8.1E-01	-2.6E-02	1.9E-01
Circular economy Conventional vehicle	3.2E-06	1.0E+00	1.6E-02	1.5E-01
Circular economy SBC vehicle	-4.0E-06	-7.2E-01	-1.7E-02	-2.2E-01
Circular bioeconomy Conventional vehicle	8.0E-06	1.3E+00	2.5E-02	4.4E-01
Circular bioeconomy SBC vehicle	-7.3E-06	-8.8E-01	-2.6E-02	1.6E-01

Note that the terrestrial acidification for the bio-based fibres (and thus also the bioeconomy futures) likely is overestimated due to uncertainties in the emission of ammonia during the lignin-based carbon fibre production. This is because nitrogen is present in the PAN molecule and not in the lignin molecule. However, as nitrogen is also used to create an inert environment, more research is needed to quantify the emissions from the carbonization and stabilization of lignin. While not as obvious for ozone depletion, these results should also be carefully viewed as we lack emissions data for many manufacturing processes.

References

- Albemarle. (2018). Lithium bis-(oxalato)borate - LiBOB (abg), advanced battery grade. Retrieved from <https://www.albemarle.com/storage/components/T408507.PDF>
- Auzanneau, F. (2013). Wire troubleshooting and diagnosis: Review and perspectives. *Progress In Electromagnetics Research B*, 49, 253-279. doi:<http://dx.doi.org/10.2528/PIERB13020115>
- AZO Materials. (n.d.). Aluminum - Advantages and properties of aluminum. Retrieved from <https://www.azom.com/properties.aspx?ArticleID=1446>
- Bhatia, S., Angra, S., & Khan, S. (2019). *Mechanical and wear properties of epoxy matrix composite reinforced with varying ratios of solid glass microspheres*. Paper presented at the Journal of Physics: Conference Series.
- ChemBK. (n.d.). Ethylene carbonate. Retrieved from <https://www.chembk.com/en/chem/Ethylene%20carbonate>
- Das, S. (2011). Life cycle assessment of carbon fiber-reinforced polymer composites. *Int J Life Cycle Assess*, 16(3), 268-282. doi:<https://doi.org/10.1007/s11367-011-0264-z>
- Dunn, J. B., James, C., Gaines, L., Gallagher, K., Dai, Q., & Kelly, J. C. (2015). *Material and Energy Flows in the Production of Cathode and Anode Materials for Lithium Ion Batteries*. Retrieved from United States: <https://www.osti.gov/biblio/1224963>
<https://www.osti.gov/servlets/purl/1224963>
- Eurocode. (n.d.). Table of design material properties for structural steel. Retrieved from <https://eurocodeapplied.com/design/en1993/steel-design-properties>
- Fazio, S., & Pennington, D. (2005). *Polyacrylonitrile fibres (PAN); from acrylonitrile and methacrylate; production mix, at plant; PAN without additives (Location: EU-27)*. European Commission, Joint Research Centre (JRC). Retrieved from: <https://data.jrc.ec.europa.eu/dataset/jrc-eplca-db00901a-338f-11dd-bd11-0800200c9a66>
- Flexicon. (n.d.). Carbon black. Retrieved from <https://www.flexicon.com/Materials-Handled/Carbon-Black.html>
- Guidechem. (n.d.). Polyvinylidene fluoride 24937-79-9. Retrieved from <https://www.guidechem.com/dictionary/en/24937-79-9.html>
- Harnden, R., Carlstedt, D., Zenkert, D., & Lindbergh, G. (2022). Multifunctional Carbon Fiber Composites: A Structural, Energy Harvesting, Strain-Sensing Material. *ACS Applied Materials & Interfaces*, 14(29), 33871-33880. doi:<https://doi.org/10.1021/acsami.2c08375>
- Hermansson, F., Ekvall, T., Janssen, M., & Svanström, M. (2022a). Allocation in recycling of composites - the case of life cycle assessment of products from carbon fiber composites. *Int J Life Cycle Assess*, 27(3), 419-432. doi:<https://doi.org/10.1007/s11367-022-02039-8>

- Hermansson, F., Heimersson, S., Janssen, M., & Svanström, M. (2022b). Can carbon fiber composites have a lower environmental impact than fiberglass? *Resources, Conservation and Recycling*, *181*, 106234.
doi:<https://doi.org/10.1016/j.resconrec.2022.106234>
- Johannisson, W., Carlstedt, D., Nasiri, A., Buggisch, C., Linde, P., Zenkert, D., Asp, L. E., Lindbergh, G., & Fiedler, B. (2021). A screen-printing method for manufacturing of current collectors for structural batteries. *Multifunctional Materials*, *4*(3), 035002.
doi:<https://doi.org/10.1088/2399-7532/ac2046>
- Johannisson, W., Zackrisson, M., Jönsson, C., Zenkert, D., & Lindbergh, G. (2019a). *Modelling and design of structural batteries with life cycle assessment*. Paper presented at the 22nd International Conference on Composite Materials (ICCM22).
- Johannisson, W., Zenkert, D., & Lindbergh, G. (2019b). Model of a structural battery and its potential for system level mass savings. *Multifunctional Materials*, *2*(3), 035002.
doi:<https://doi.org/10.1088/2399-7532/ab3bdd>
- Kim, H., Guccini, V., Lu, H., Salazar-Alvarez, G. n., Lindbergh, G. r., & Cornell, A. (2018). Lithium ion battery separators based on carboxylated cellulose nanofibers from wood. *ACS Applied Energy Materials*, *2*(2), 1241-1250.
doi:<https://doi.org/10.1021/acsaem.8b01797>
- Lam, S. S., Azwar, E., Peng, W., Tsang, Y. F., Ma, N. L., Liu, Z., Park, Y.-K., & Kwon, E. E. (2019). Cleaner conversion of bamboo into carbon fibre with favourable physicochemical and capacitive properties via microwave pyrolysis combining with solvent extraction and chemical impregnation. *J Clean Prod*, *236*, 117692.
doi:<https://doi.org/10.1016/j.jclepro.2019.117692>
- Lv, D., Chai, J., Wang, P., Zhu, L., Liu, C., Nie, S., Li, B., & Cui, G. (2021). Pure cellulose lithium-ion battery separator with tunable pore size and improved working stability by cellulose nanofibrils. *Carbohydr. Polym.*, *251*, 116975.
doi:<https://doi.org/10.1016/j.carbpol.2020.116975>
- Materials Project. (n.d.). LiFePO₄. Retrieved from https://materialsproject.org/materials/mp-19017#how_to_cite
- Moncada, J., Gursel, I. V., Huijgen, W. J., Dijkstra, J. W., & Ramírez, A. (2018). Techno-economic and ex-ante environmental assessment of C₆ sugars production from spruce and corn. Comparison of organosolv and wet milling technologies. *J Clean Prod*, *170*, 610-624. doi:<https://doi.org/10.1016/j.jclepro.2017.09.195>
- Romaniw, Y. A. (2013). *The relationship between light-weighting with carbon fiber reinforced polymers and the life cycle environmental impacts of orbital launch rockets*. Georgia Institute of Technology,
- Royal Society of Chemistry. Copper. Retrieved from <https://www.rsc.org/periodic-table/element/29/copper>
- Sigma-Aldrich. (n.d.-a). 2,2'-Azobis(2-methylpropionitrile) solution. Retrieved from <https://www.sigmaaldrich.com/SE/en/product/aldrich/714887>

- Sigma-Aldrich. (n.d.-b). Bisphenol A ethoxylate dimethacrylate. Retrieved from <https://www.sigmaaldrich.com/SE/en/product/aldrich/455059>
- Sigma-Aldrich. (n.d.-c). Propylene carbonate. Retrieved from <https://www.sigmaaldrich.com/SE/en/product/sigald/p52652>
- Stanford Advanced Materials. (n.d.). LM3791 Lithium Trifluoromethanesulfonate (LiTf) (CAS No.33454-82-9). Retrieved from <https://www.samaterials.com/lithium-trifluoromethanesulfonate-litf.html>
- Tasneem, S., & Siam Siraj, M. (2022). Improvements in structural battery cells processing: manufacture, characterization, and multicell demonstration.
- Thyssenkrupp. (2022). Density of Aluminium. Retrieved from <https://www.thyssenkrupp-materials.co.uk/density-of-aluminium.html>
- Zackrisson, M., Avellán, L., & Orlenius, J. (2010). Life cycle assessment of lithium-ion batteries for plug-in hybrid electric vehicles – Critical issues. *J Clean Prod*, 18(15), 1519-1529. doi:<https://doi.org/10.1016/j.jclepro.2010.06.004>
- Zackrisson, M., Jönsson, C., Johannisson, W., Fransson, K., Posner, S., Zenkert, D., & Lindbergh, G. (2019). Prospective Life Cycle Assessment of a Structural Battery. *Sustainability*, 11(20), 5679. doi:<https://doi.org/10.3390/su11205679>